QUARTERLY PROGRESS REPORT NO. 3

EFFECTS OF NEUTRON DAMAGE ON THE MECHANICAL PROPERTIES OF PYROLYTIC AND SINGLE CRYSTAL GRAPHITE

October 1, 1964 to December 31, 1964

Principal Investigator

J. T. Meers

UNION CARBIDE CORPORATION
CARBON PRODUCTS DIVISION, RESEARCH LABORATORY

This program has been jointly supported by the
United States Atomic Energy Commission
Contract No. AT-(40-1)-3237
and
Union Carbide Corporation

Parma, Ohio 44130

July 26, 1965

DISCLAIMER

FOREWORD

This report summarizes the progress of an investigation of the effects of neutron damage on the mechanical properties of both graphite single crystals and pyrolytic graphite which has been compression annealed. The work is jointly supported by the United States Atomic Energy Commission under Contract No. AT-(40-1)-3237 and Union Carbide Corporation, Carbon Products Division. The Contract is administered by Dr. D. F. Cope, Director, Reactor Division, Oak Ridge Operations. The report covers the period October 1, 1964 to December 31, 1964.

The Project is under the general supervision of J. T. Meers. The graphite single crystal work has been carried out by R. Sprague, R. Bacon, D. E. Soule, and C. W. Nezbeda. The pyrolytic graphite work has been carried out by O. L. Blakslee, D. G. Proctor, E. J. Seldin, G. B. Spence, and T. Weng. The X-ray analyses were made by C. E. Lowell. This report was prepared by J. T. Meers with the assistance of the participants in the program.

ABSTRACT

Materials for the test program have been prepared; these include natural graphite crystals and compression-annealed pyrolytic graphite. The shear strength of compression-annealed pyrolytic graphite has been measured, and values ranging from 150 to 350 psi were observed. An apparatus for the static torsion testing of compression-annealed pyrolytic graphite has been constructed. Work has been continued on the measurement of the elastic stiffness and compliance constants. Timoshenko's equation for the flexural vibrations of a long thin bar has been solved, and the solution is being used to compute the value of one modulus from the measured resonant frequency and a known value of the other modulus. To make this computation economical for a large number of bars, a program was written for a digital computer. One plane of vibration yields a value of Young's modulus $1/s_{11}$; the other plane of vibration gives the shear modulus $1/s_{44}$.

TABLE OF CONTENTS

TABLE OF CONTENTS

LIST OF ILLUSTRATIONS

LIST OF TABLES

1. INTRODUCTION

The general objective of the program is to determine the effects of neutron irradiation upon the mechanical properties of graphite single crystals and of highly ordered pyrolytic graphite. The specific objective of the first year's work has been the production and pre-irradiation evaluation of these materials.

In the first two quarterly reports,[1,2] methods of production and evaluation of these graphites were described. As the work has progressed, difficulties experienced with the control of the growth of graphite crystals led to the alternative of obtaining naturally occurring crystals. Compression-annealed pyrolytic graphite of good quality has been produced, and the problem remaining with the process appears to be that of scale up to larger dimensions.

Because of the severe anisotropy, mechanical property measurements on highly ordered pyrolytic and single crystal graphite are very much more difficult than on ordinary materials. The small size of available single crystals presents additional problems. In order to insure confidence in the correctness of the measured values, it was planned that, during the first year's effort, almost every property would be measured by more than one method. Work during the third quarter has been mainly on developing the various individual tests. In particular, work has been continued on improving the static tensile tests of pyrolytic and single crystal graphite. More shear strength measurements on pyrolytic graphite were made, and exploratory work on the shear strength of single crystals was started. An apparatus to measure the stress-strain curve in torsion on pyrolytic graphite has been constructed. The computer program to calculate the shear modulus from flexural vibrations of a resonant bar has been completed and put into operation.

2. SUMMARY

Work to obtain a supply of graphite crystals and good quality compression-annealed pyrolytic graphite has proceeded satisfactorily. A supply of natural graphite crystals was obtained by acid dissolving calcite which contained graphite

crystals. This calcite was obtained from Essex County, New York. Disks of stress-annealed pyrolytic with diameters up to two and one-half inches were produced. The quality of the pyrolytic has been evaluated by optical reflectance and X-ray techniques; these tests have been developed into a routine technique. A third furnace load of special pyrolytic graphite has been ordered and received.

Several exploratory tests were conducted to measure the between-planes shear strength of graphite single crystals. These tests have demonstrated the feasibility of measuring the shear strength of single crystals, and an improved apparatus is being designed for this measurement. An apparatus has been constructed during this period which will measure the torsional properties of small disks of pyrolytic graphite. The shear strength and the torsional stress-strain relationship can thus be obtained. The shear strength of pyrolytic graphite has been measured using compression shear wedges. Shear strengths ranging from 150 to 350 psi were obtained for stress-annealed pyrolytic graphite by extrapolating measured values to the limit of zero normal force. Work has been continued on the problem of measuring static compression and tensile properties of stress-annealed pyrolytic graphite. Consistent values of $1/s_{11}$ have not been obtained in either flexure or tension, but the problem has been defined as nonuniform stress distribution across the thickness of the specimen.

Timoshenko's equation for the flexural vibrations of a long thin bar has been solved, and the applicability of the solution for isotropic and anisotropic materials has been tested. It is shown that for near-isotropic bodies with a relatively high G/E (shear to Young's modulus) ratio only Young's modulus can be determined accurately from flexural vibrations of a bar. For compression-annealed graphite with a very low shear modulus compared to Young's modulus, only the shear modulus can be calculated from flexural vibrations of a bar.

The dependence of the Timoshenko constant, k, upon both the harmonic number and the cross-sectional shape has been investigated for nearly isotropic materials, and two important conclusions have been drawn. First, to within one per cent variation, the value of k is independent of harmonic number (at least up to n = 3) and of the length to diameter ratio. Second, as G/E increases from $^1/_3$ to $^1/_2$, the value of k decreases monotonically. The analysis of the vibrational frequencies of isotropic square bars gives a value of k which is

significantly less than the theoretical value for a round bar with the same value of G/E. By extrapolating the results for several materials, a value of $k = 0.85 \pm .05$ is indicated for rectangular bars of compression-annealed pyrolytic graphite, and this value of k should apply to all harmonics, to all reasonable values of the D/T and D/L ratios, and to varying amounts of anisotropy.

Up to this time, only a few measurements of c_{44} have been made by different test methods on either the same sample or on adjacent samples from the same disk. These preliminary results indicate that the values of c_{44} obtained by ultrasonics, the compound torsion oscillator, and the first 5 to 10 flexural harmonics and the first torsional vibration of a resonant bar are all within about 15 per cent of one another and, sometimes, within about 5 per cent. It appears that c_{44} may vary by 10 to 20 per cent for different layers from the same disk. However, values of c_{44} measured on samples taken from different disks have varied by as much as a factor of 2, from roughly 0.017 to 0.034×10^{11} d/cm^2. In view of the expected tenfold increase in c_{44} after neutron irradiation, it appears that the accuracy of the measurements is satisfactory but that pre- and post-irradiation measurements will have to be made on the same sample or, at least, on samples from the same disk.

3. MATERIALS PREPARATION

Early in this quarter, a decision was made to explore the possibility of obtaining a supply of natural crystals, and work on the growth of graphite single crystals was discontinued. The annealing of pyrolytic graphite continues to be a problem; and, although good material has been produced occasionally, the causes and effects have not been related in a completely satisfactory way.

3.1. Single Crystals

G. Wagoner, D. E. Soule

A series of experiments was made with iron-carbon systems held at temperatures at or near 2675°C for times up to 30 hours. The crystals, when produced, were of good quality but small; the occasional large crystals were invariably so thin that they were severely damaged by removal from the crucible. As a result, crystal growing was discontinued, and attention was

directed toward obtaining naturally occurring single crystals of graphite. A survey of the regional distribution of natural graphite deposits, prepared by Cameron and Weis,[3] was helpful for this purpose.

Essex County, New York, has been a particularly fruitful area for obtaining natural graphite crystals, and a screening evaluation of marble, quartz, calcite, and granites from Essex County had been made in August of 1964. The graphite crystals found in calcite were of the best quality; and, when the decision was made to obtain natural graphite crystals, a quantity of Essex County calcite was obtained. The crystals were recovered by acid leaching. A typical array of crystals from a fist-size piece of calcite is shown in Figure 1. The crystals were then washed, dried, and purified in a stream of gaseous chlorine at 3000°C. Since this last step can be destructive if a furnace element breaks, only a few crystals were processed per run. These purification runs will be continued until the crystals are all purified.

3.2. Compression Annealing of Pyrolytic Graphite

It was established during the first two quarters that the best conditions for annealing pyrolytic graphite depended upon its growth structure. For example, at 2800°C and 8000 psi, ordinary commercial pyrolytic graphite anneals without side slipping. However, when pyrolytic graphite was made with greatly reduced numbers of soot inclusions, these conditions were too severe and side slipping did occur.

A series of experiments was performed to determine the best conditions of pressure and temperature for annealing special propane and methane deposited graphite. The plate diameter was reduced to 1.5 inches for these tests, and experiments were carried out at temperatures and pressures which ranged from 2650°C to 3400°C and 1000 to 8000 psi, respectively. The best annealing conditions for propane deposited material were found to be 2800°C and 4000 psi. The propane base material slightly side slipped under these conditions, but weaker conditions are not sufficient to straighten the layer planes. Several pieces were given an additional anneal at temperatures of 3350°C while under a pressure of 800 psi; the additional heat treatment did not cause marked changes in the material.

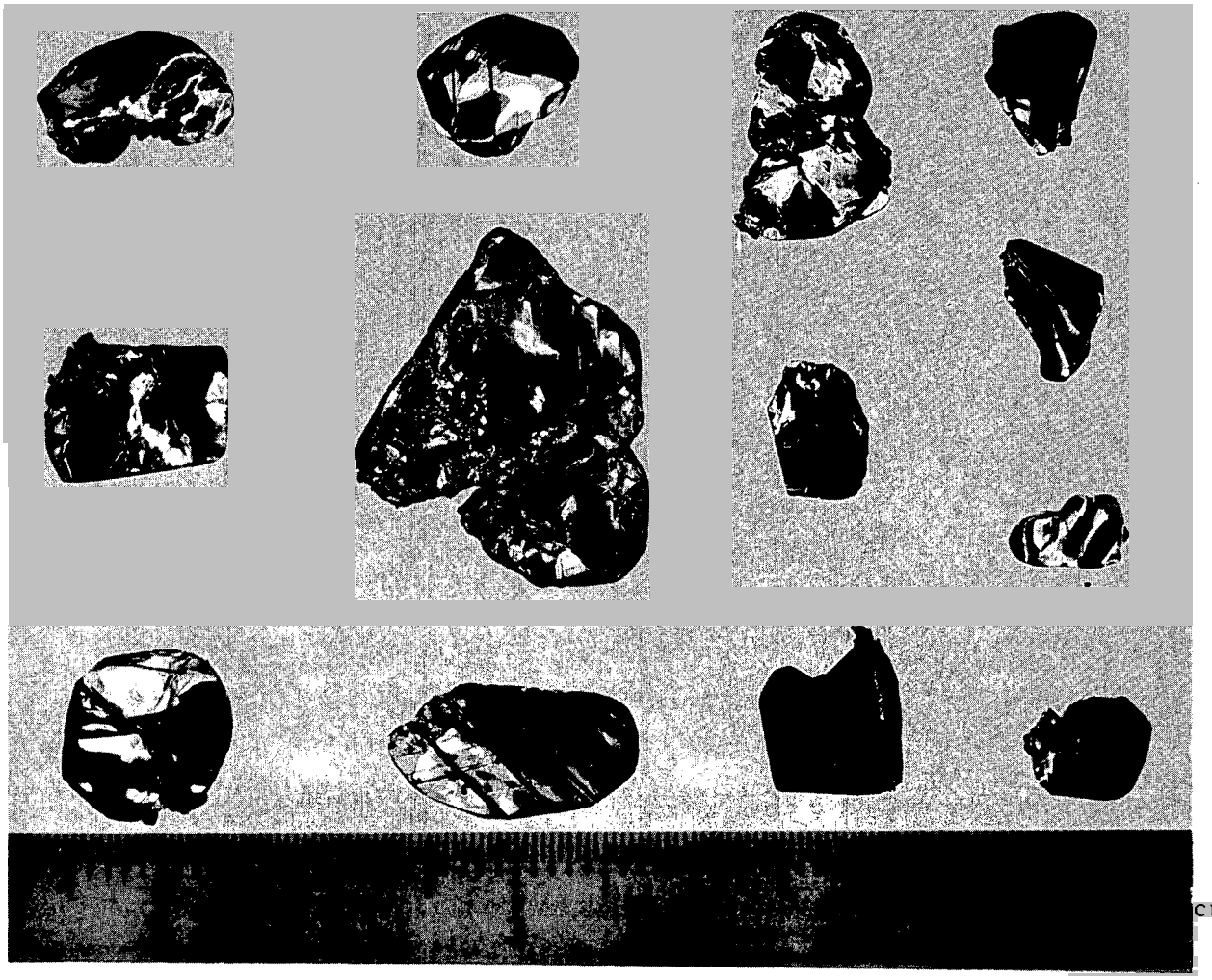

FIGURE 1. Natural Graphite Crystals Obtained from Calcite.

N-6271

After stress-annealing conditions were established for 1.5 inch diameter disks of pyrolytic graphite, the sample size was increased to 2.5 inches. These larger samples of propane material also showed a slight tendency to side slip. A thermal anneal at 3350° C and 500 psi did not produce any noticeable improvement. As reported in the following section, the optical reflectivity half-widths of the crystallite orientation distributions for the material annealed during this period have been in the range 0.2 to 0.7 degree, except for poorer material near the surfaces of the disks. These favorable results have led to the decision to scale up to 3.5 inches sample size during the next quarter.

3.3. Third Order of As-Deposited Pyrolytic Graphite

During this quarter, a third furnace load of pyrolytic graphite had to be ordered. Before specifying the material for this order, a basic question had to be resolved. It had been found by optical microscopy that the previous propane material had less soot but more internal delaminations than the methane material. The high misorientation around soot particles tends to lock the layer planes together; thus, when the amount of soot is reduced, delaminations become more frequent. The contract objective of producing pyrolytic graphite representative of the natural graphite single crystal requires the elimination of as much soot as possible. However, it was feared the increased delaminations of the as-deposited soot-free material might so weaken the material after compression annealing that meaningful mechanical property measurements could not be made.

To investigate this question, samples from the previous methane and propane furnace runs were simultaneously compression annealed by placing two or three disks in the load train with ZTA grade graphite spacers between the disks. This procedure eliminated the possibility of any differences in the final material being due to variations in pressing conditions. Next, the shear strength was measured on samples cut from the methane and propane disks; it was felt that the shear strength would be more critically affected by delaminations than any other property. From the results of these tests (reported in Section 6), no significant difference due to the starting material could be found between the methane and propane material. Consequently, it was decided to order fine-grain substrate nucleated pyrolytic graphite similar to the propane material. Engineers at High Temperature Materials, Inc., suggested that

methane gas be used, but with different manufacturing conditions than those which had been used for the first furnace load made with methane. In view of the previous failure to attain high quality by compression-annealing 5-inch diameter plates, it was decided to place the order for 3 to 3.5-inch diameter plates.

Twenty-five plates were made approximately 3.5 inches in diameter and about $^3/_8$ inch in thickness. In accordance with our numbering system, these plates made from methane in the third furnace will be designated M301 to M325. Plate M301 was shipped to the Research Laboratory at Parma, Ohio, for evaluation of the as-deposited material. The remaining 24 plates were shipped to the Advanced Materials Laboratory at Lawrenceburg, Tennessee, for compression annealing after the compression-annealing process has been scaled up. As discussed in Section 4.2., the structure of this new material seems to be very close to that desired.

4. MATERIAL CHARACTERIZATION

Optical reflectivity, optical interferometric, and X-ray techniques have been used to evaluate the crystallite orientation distribution of compression-annealed pyrolytic graphite. Because the optical reflectivity method is quicker, less expensive, and applicable to samples prepared for mechanical property measurements, this technique has been adopted as a screening device. However, there appears to be a systematic difference between the results obtained by optical and X-ray methods. This point is discussed in the following section.

The structure of the material from the third furnace of pyrolytic graphite has been investigated by optical microscopy; the results are discussed in Section 4.2. The investigation of the failure of the cathodic etch to reveal grain boundaries on some specimens of compression-annealed pyrolytic graphite has continued but without definitive results. It is presently thought that impurities were responsible for the cathodic etching of grain boundaries; this hypothesis will be tested.

4.1. Comparison of Optical Reflectivity and X-ray Methods

O. L. Blakslee and C. E. Lowell

By better adjustment of the optical reflectivity apparatus, the limit of resolution has been improved. The half-width at half-height of the angular distribution obtained with a plane mirror is now less than 0.1 degree.

The half-width at half-height, $\theta_{1/2}$, of the crystallite orientation distribution has been measured by X-rays on the as-deposited sample M301-2 from the third furnace; the values from 22 to 24° are in the same range as those obtained on the previous material. As a matter of curiosity, the distribution was measured optically on the unmachined c-face of the same sample: a value of 7.1° was obtained. The optical method may not be reliable on the dull as-deposited surface, but the results seem reasonable in that X-rays will detect smaller crystallites and the smaller crystallites are probably more misoriented.

The X-ray and optical reflectivity methods of measuring the crystallite orientation distribution of the compression-annealed material have been compared by measuring several samples by both methods. The X-ray and optical values of $\theta_{1/2}$ and the ratio of these values are given in Table 1. The X-ray value is usually about twice the optical value, but the ratio varied from 1.1 to 2.9. There are several reasons why the X-ray and optical results could differ. The instrumental broadening in the X-ray method may be greater for graphite than estimated from measurements on an MgO crystal (0.05 degree). Alternatively, the X-ray distribution may actually be different from the optical distribution because of the difference in wave lengths (smaller crystallites contribute to the X-ray beam) and because the X-ray beam penetrates approximately 0.02 inch and measures a volume rather than a surface distribution. Soot particles seem to broaden the optical distribution, presumably by diffraction effects. It is felt that this diffraction broadening is not important in the propane-deposited material but is present in the upper half of the first methane-deposited material and in most commercial-quality material.

Further work is necessary if the significance of the X-ray and optical results is to be understood. On well-annealed material, either method can be reliably used to compare the degree of crystallite alignment of different samples. On poorer quality material, the X-ray method is preferred.

TABLE 1

CRYSTALLITE ORIENTATION DISTRIBUTION
HALF-WIDTH AT HALF-HEIGHT

Sample	Method		Ratio
	Optical	X-ray	X-ray/Optical
M110-2	0.18	0.52	2.9
M110-3	.38	.78	2.1
P210-3	.20	.38	1.9
M110-4A	.57	.83	1.5
M110-4B	.32	.64	2.0
P210-4A	.65	.71	1.1
P210-4B	.21	.34	1.6
M110-5	.42	.76	1.8
P210-5	.27	.61	2.3
P210-6	.22	.43	1.9
M111-1	.51	.72	1.4
P211-1	.29	.53	1.8

4.2. Evaluation of the Third Order of As-Deposited Pyrolytic Graphite

Plate M301 from the third special order of pyrolytic graphite has been examined by optical microscopy. Figure 2 shows the structure near the center layers of the plate. The material has a uniform fine grain, substrate nucleated structure from the bottom to the top of the plate, a structure very similar to that of the propane-deposited material. This plate had one large delamination just above the area shown in Figure 2 but has very few of the small microcracks found in the propane material. The average cone size is slightly smaller than that of the previous materials, and the density (2.16 g/cm^3) and crystallite distribution are similar to the properties of the previous materials. The third order of pyrolytic graphite appears to be the best yet produced and should be satisfactory for the purpose of the program.

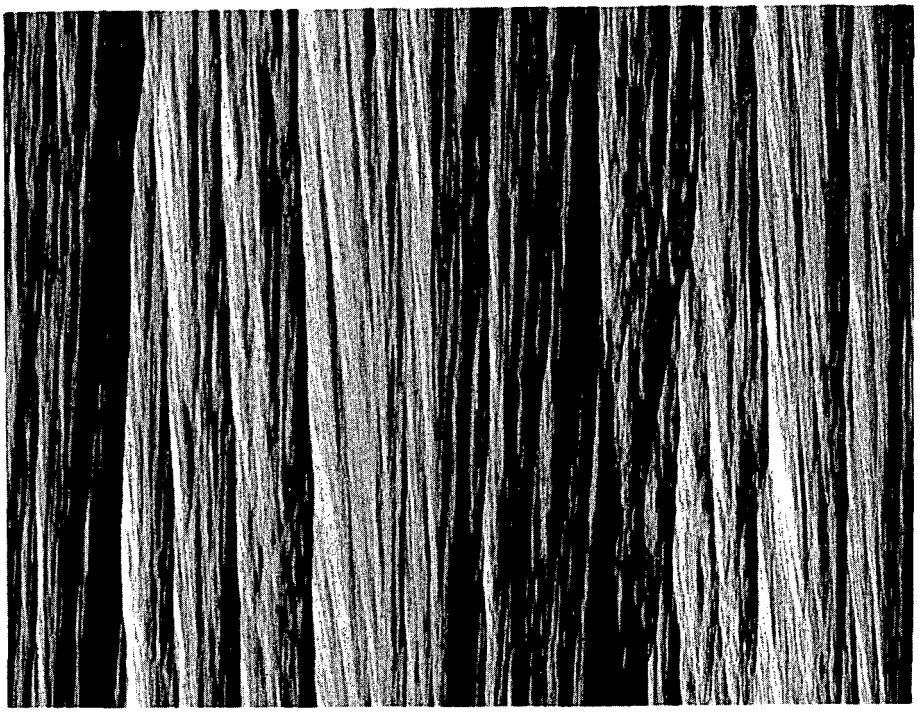

FIGURE 2. Fine Grain, Substrate Nucleated Structure of As-Deposited Methane Disk M301. Magnification 75X.

5. STATIC TESTS OF GRAPHITE SINGLE CRYSTALS

5.1. Preparation of Tensile Specimens

R. Sprague

A number of techniques for the preparation of single crystal tensile specimens were tried. Two methods were unsatisfactory: air abrasive shaping of the sample with a single mask caused cavitation and disruption of the edges of the sample; properly shaped samples were punched from a copper plated crystal, but the plating did not prevent disruption of the sample edge.

A third method originated by D. E. Soule[4] was very successful. The crystal or material to be cut is sandwiched between two identical templates and the sample is cut out with an abrasive jet. Care must be taken to direct the jet stream so as to prevent rebounding particles from undercutting the templates.

5.2. Test Apparatus

R. Bacon

The microtest machine for graphite single crystals is under construction in the laboratory apparatus shop.

5.3. Basal Plane Shear of Graphite Single Crystals

D. E. Soule, E. J. Seldin, and T. Weng

Crude shear tests were made on two small natural single crystals of graphite with areas of 13.2 mm^2 and 21.2 mm^2, respectively. The specimen in each test was cemented with Duco cement between two thin strips of a hard plastic. The upper strip was held in a vise and the lower strip was weighted with a metal can into which water was gently poured until the specimen broke. The values of shear strength for each specimen are given in Table 2.

TABLE 2

SHEAR STRENGTH OF GRAPHITE SINGLE CRYSTALS

Sample	Trial	Glue Contact	Shear Force g	Shear Strength g/mm^2	Shear Strength $lb/in.^2$
A	1	imperfect	1140	86	122
	2	good	1640	124	176
B	1	good	2590	122	174
	2	imperfect	2340	110	156

These preliminary results are in the range of shear strengths (120 to 360 $lb/in.^2$) measured in stress-annealed pyrolytic graphite but are higher than the 40 to 50 g/mm^2 (57 to 71 $lb/in.^2$) reported by L. M. Gillin.[5] The results show that it is possible to measure with some accuracy shear in the basal plane. An apparatus designed for measuring the shear strength of graphite single crystals is now under construction.

6. STATIC TESTS ON PYROLYTIC GRAPHITE

E. J. Seldin and T. Weng

Some routine compression tests were run on as-deposited pyrolytic graphite from the new furnace load of material in order to obtain elastic constants and to characterize the base stock. Tension tests were run on a single specimen of stress-annealed pyrolytic, the ends of which were potted in epoxy resin in order to investigate the influence of the end grips on the measurement of strain on the a- and c-faces of the specimen; the tests give evidence of a nonuniform stress distribution along the c-axis, the nonuniformity becoming greater as the amount of specimen surface in contact with the epoxy is increased. As a check on the value of the modulus $1/s_{11}$ obtained in tension, this modulus was also determined by means of a flexure test; the value obtained in flexure is in the middle of the range of values obtained thus far in tension. A torsion apparatus has been constructed which will be used to obtain static stress-strain curves and to evaluate s_{44}. The shear tests, using compression-shear fixtures, have been continued, and considerable variation has been found among different stress-annealed graphites.

6.1. Results of Compression Tests on As-Deposited Pyrolytic Graphite

A representative disk of as-deposited methane base pyrolytic graphite from the third furnace load of material was evaluated. The purity of the material, as obtained from spectrographic analysis, was comparable to that of the best material tested so far, with only trace elements of impurities. Three specimens from this disk (M301) were tested in compression. The elastic moduli which were determined are given in Table 3. The moduli are typical of those obtained with other as-deposited pyrolytic graphites.

6.2. Results of Tensile Tests on Compression-Annealed Pyrolytic Graphite

A series of tensile tests on one specimen of compression-annealed pyrolytic graphite was performed to check the influence of the epoxy end pieces on the determination of the elastic modulus. All previous tensile tests on specimens with ends potted in epoxy resin had yielded the following result: the strain measured with strain gages on the c-faces of the specimen was consistently greater than the strain measured with strain gages on the a-faces. The explanation of this odd behavior was hypothesized: the outer

TABLE 3

ELASTIC CONSTANTS OF AS-DEPOSITED PYROLYTIC GRAPHITE FROM COMPRESSION TESTS

Sample	Young's Modulus (10^6 lb/in.^{2})		Compliance Constants (10^{-12} cm^2/d)			Poisson's Ratio
	$1/s_{11}$	$1/s_{33}$	s_{11}	s_{33}	s_{13}	$-s_{13}/s_{33}$
M301-6	3.70*		3.92			
M301-7		1.70		8.55	-3.06	.36
M301-8		1.59		11.0	-3.09	.28

* Gages mounted on c-face.

c-faces of the specimen are bonded to the epoxy within the end pieces. Since the modulus of the epoxy is very small (0.5×10^6 lb/in.^{2}) compared with $1/s_{11}$ for the graphite, the epoxy undergoes a relatively high strain, which is communicated to the c-faces of the graphite. However, because of the low shear modulus of the graphite, the strain decreases from a high value on the outer surfaces to a lower value within the material. Therefore, the gages on the outer c-faces detect a high strain and the gages on the a-faces detect a lower strain. A series of tests were performed in order to check this hypothesis.

The tests are summarized in Table 4. The specimen (C5-16) of the type shown in the Second Quarterly Progress Report[6] was 0.136 inch thick, 2.75 inches long, 0.5 inch wide on each end, and had a gage section 0.25 inch wide by 1.5 inches long. For the first test, the epoxy end pieces left an effective gage length of I inch. The ratio of the strain measured on the c-faces to that measured on the a-faces was slightly greater than two-to-one. Table 4 lists the modulus as determined by dividing the average stress by the strains measured on either the c- or a-faces.

After the first test, approximately $^3/_8$ inch of each epoxy end piece was cut away from the main part of the piece by undercutting on a band saw. The small pieces which were cut away remained in contact with the

graphite; but, since they were not under any appreciable stress when the load was applied, the effective gage length of the specimen was increased to about 1.5 inches. As a result, the strains which are measured on the a- and c-faces on the second tensile test were less unequal, although the measured strain was still greater on the c-faces than on the a-faces.

In an attempt to reduce shear effects across the width of the specimen, a $^{7}/_{64}$ inch diameter hole was drilled through the epoxy and each end of the specimen, and a steel pin was inserted for the third test. The results of the third test were similar to those of the second test. The steel pins in the ends did not appear to influence the stress distribution, but the holes in the ends tended to weaken the specimen for the next tests.

After the third test, the epoxy end pieces were cut away completely from the specimen. Because the ends of the specimen were also slightly undercut, some material was cleaved from each side of the specimen until both c-faces were smooth and unmarred. Aluminum foil was then attached to the c-faces on both ends of the specimen with rubber cement, which forms a relatively weak bond between the aluminum and graphite. New epoxy end pieces were then potted on each end of the specimen, but this time the epoxy bonded to the aluminum foil instead of to the graphite. On the fourth test, the strains measured on the a- and c-faces were more nearly alike than any obtained previously; however, there was still some uncertainty in the results in that the specimen appeared to break slightly at one end at a stress of 3000 lb/in.^{2} For the stress-strain curves obtained with the gages on the a-faces, the slope of the curve on increasing the load was slightly different from the slope obtained on decreasing the load. When the load was reapplied, the stress reached 4200 lb/in.^{2} before the stress-strain curve indicated a break; but this time, the measured strain was greater on the c-faces than on the a-faces. These tests indicate that the value of the elastic modulus $1/s_{11}$ for this sample is approximately 130 to 135 x 10^6 lb/in.^{2}

This series of tests shows that the original hypothesis is correct. The experimental problem which must be solved is that of obtaining a uniform-stress distribution across the width of the specimen. Since the epoxy end pieces cause great difficulty, other methods of gripping the ends of the specimen will be tried.

TABLE 4

RESULTS OF TENSILE TESTS OF COMPRESSION-ANNEALED PYROLYTIC GRAPHITE

Test No.	Initial Condition of Specimen No. C5-16	Modulus (10^6 lb/in.^{2}) As Measured by Gages on c-faces	Modulus (10^6 lb/in.^{2}) As Measured by Gages on a-faces	Comments
1	Epoxy contacting c-faces at ends; 1 inch long gage-section.	76	165	To 5850 psi max. Stress-strain curves linear. Thickness = .136 inch.
2	Undercut epoxy $^3/_8$ inch from each end; $1^3/_4$ inches long effective gage section.	111	149	To 5850 psi max. Curves not linear on first application of load; linear thereafter.
3	Pinned each end with $^7/_{64}$ inch diameter steel pin through epoxy.	114	155	To 5850 psi max. Curves linear
	Removed specimen from epoxy and cleaved material from c-faces to make thinner specimen.			Thickness = .103 inch.
4a	Ends of specimen within epoxy covered with aluminum foil.	135 134	125 141	Load applied. Load removed. Slipping observed at 3000 psi believed to be due to cracking at one end of specimen. Curves fairly linear.
4b	Same as above, but one end of specimen broke slightly inside epoxy.	126	144	To 4200 psi. More slipping was observed. Curves fairly linear.

6.3. Results of Flexure Tests on Compression-Annealed Pyrolytic Graphite

A flexure test using 4-point loading was made on a bar of compression-annealed pyrolytic graphite (C5-61) measuring 0.282 inch on the c-face, 0.137 inch on the a-face, and a little over 3 inches in length. The loading rollers were spaced 3 inches apart on one side of the bar and 1.5 inches apart on the other side. The load was applied perpendicular to the c-direction, and gages were placed on both of the a-faces in the center of the specimen to measure the tensile and compressive strains. The value of $1/s_{11}$, determined from both of the strain measurements, was 117 x 10^6 lb/in.^{2}

The reason for making the flexural test was to see which of the wide range* (76 to 175 x 10^6 lb/in.^{2}) of tensile values of $1/s_{11}$ is correct. The flexural value of 117 falls near the middle of the tensile range and tends to confirm the conclusion reached in the preceding section that the very low and very high tensile values are due to a nonuniform stress distribution across the gage section. The values of 117 and 130 to 135 reported here were measured on commercial-quality material which was highly but not perfectly aligned. Presumably, the true value of $1/s_{11}$ for a perfect graphite crystal should be slightly higher.

6.4. Torsion-Test Apparatus

An apparatus has been designed and constructed during this period which will be used to perform a static-torsion test on disks of compression-annealed pyrolytic graphite. Initial tests were made on disks 0.5 inch in diameter with thicknesses of approximately 0.015 inch and larger. The strain is measured with a differential transformer, and a pure torque is obtained by applying weights in equal pairs to two strings which pass over pulleys and which are attached to a torsion wheel of known diameter. The specimen is cemented between two metal rods, and the initial tests involved trials of different cements and calculation of end effects in the apparatus. The initial tests have demonstrated that there is sufficient sensitivity to obtain stress-strain curves in torsion, and values of $1/s_{44}$ in the neighborhood of 0.02 x 10^{11} dynes/cm^2 have been obtained which are close to the values obtained in sonic and ultrasonic experiments.

6.5. Results of Shear Tests on Compression-Annealed Pyrolytic Graphite

Several stress-annealed pyrolytic graphites were tested in shear using the compression-shear fixtures described in the Second Quarterly Progress Report.[8] The four sets of fixtures had bases measuring 0.5 by 0.25 inch and shear planes making an angle θ with the horizontal of 15°, 30°, 45°, and 60°, respectively. Figure 3 is a plot of the shear stress at failure vs. the normal stress; the data points represent in each case the

---

* Data from Table 2 of the Second Quarterly Progress Report[7] and from Table 4 of this report.

average of six to ten determinations on a thin slab of material. The data are extrapolated linearly to obtain a value for the shear strength in the limit of zero-normal stress. The values which were obtained varied from 220 to 360 lb/in.^{2}

Four additional sets of compression-shear fixtures were made with the same angles but with bases measuring 0.25 by 0.25 inch. Shear tests were run using both the large and small fixtures on material from a single 0.0675 inch thick slab taken from stress-annealed graphite piece C5. Because of the relatively large thickness of the slab, one-half of the original thickness proved to be more than sufficient material for a series of tests; unfortunately, no precautions were taken to identify each half-piece. The results of the series of tests are shown in Figure 4. The data points seem to fall roughly into two groups, which we interpret to mean that the average shear strength over half of the original thickness of the slab is slightly different from the average shear strength over the other half of the slab. It seems, in addition, that the shear strength which is obtained is independent of the size of the fixtures. The shear strength of material C5 is much lower than that of any other graphite which we have thus far tested; Figure 4 indicates a value of 150 to 170 lb/in.^{2}, and previous tests showed values as low as 120 lb/in.^{2}

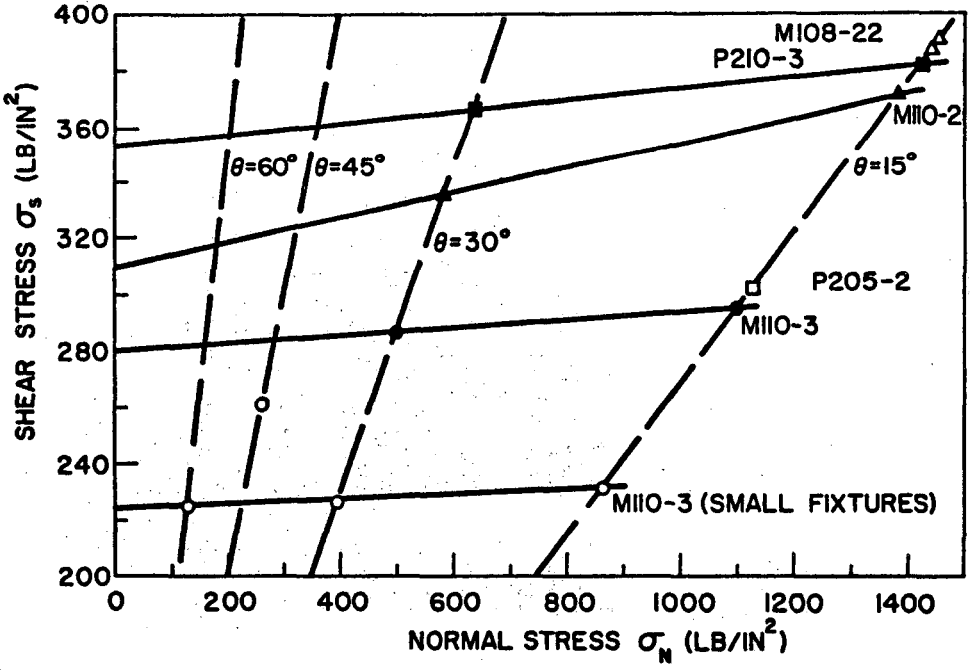

FIGURE 3. Shear Stress at Failure vs. Normal Stress for Several Compression-Annealed Pyrolytic Graphites.

N-6505

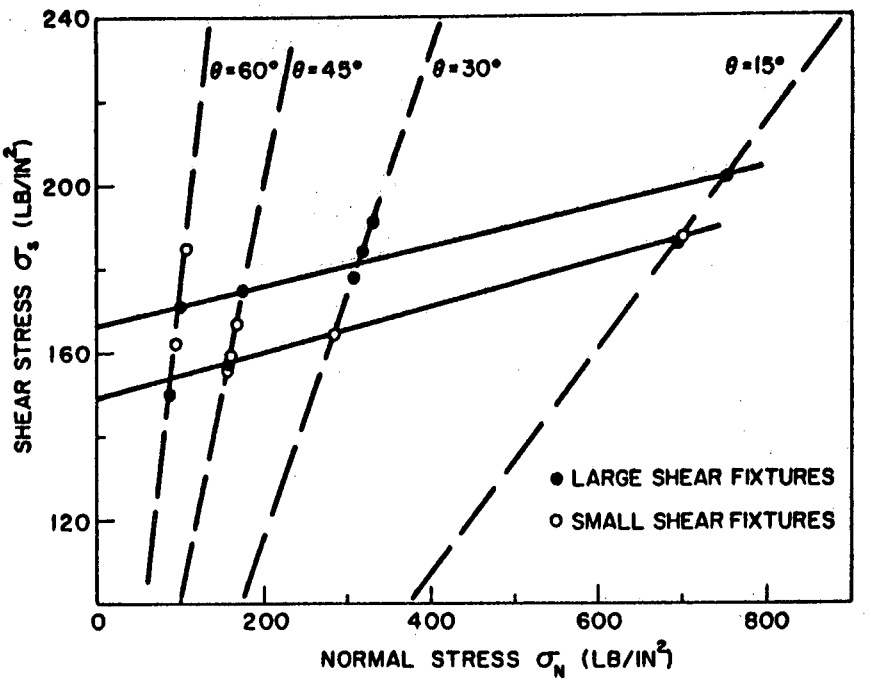

FIGURE 4. Shear Stress at Failure vs. Normal Stress for Compression-Annealed Pyrolytic Graphite C5.

N-6506

7. ULTRASONIC AND RESONANT BAR TESTS ON PYROLYTIC GRAPHITE

O. L. Blakslee, D. G. Proctor, and G. B. Spence

7.1. Sample Preparation

One change has been made in the procedure described in the Second Quarterly Report[9] for preparing the 0.5 inch disks used in the CTO experiment and in the static torsion test. Plates of ATJ graphite $^3/_{16}$ inch thick are placed between the drill rods and the stress-annealed material. The plates are machined along with the stress-annealed sample to provide support so that the grinding wheel doesn't "dogear" the edges of the layer planes. This "dogearing" was originally thought to be of no consequence, since it appeared that the damaged material was eventually machined away. However, it was found that the bending and disruption of the planes propagates injuries about 1 mm into the 0.5 inch sample disk, even though the sample is supported by the drill rods.

7.2. Resonant Bar Test

A. Resonant Bar Apparatus

A new transducer system was used with the resonant bar apparatus and found to be useful to frequencies as high as 120 kc. The transducers themselves are piezoelectric bars approximately 9 x 1.5 x 0.7 mm, operating in flexure. The particular bars used here were removed from a Weathers C-501 stereo phonograph cartridge and remounted as shown in Figure 5. It has been found that merely placing the tips of the transducer elements on a sample bar and applying approximately 4 to 5 grams of force provide sufficient mechanical coupling. Raising the frequency limit to 120 kc makes it possible to measure the fundamental longitudinal resonance on stress-annealed bars as short as 7 cm in length.

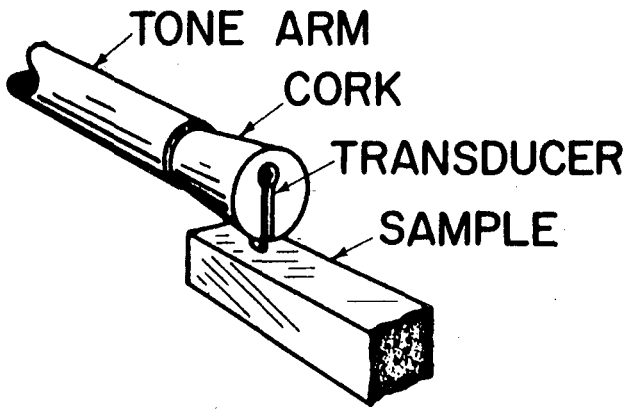

FIGURE 5. Modified High Frequency Transducer for Resonant Bar Apparatus
N-6712

B. Resonant Bar Theory: Solution of Timoshenko's Equation

Method of Solution

The flexural vibrations of a long thin bar are described rather accurately by a differential equation proposed by Timoshenko.[10] Timoshenko's contribution was to include, in an approximate way, the deformation of the bar due to the shear of one cross-section with respect to its neighbor. The solution of Timoshenko's equation for appropriate boundary conditions at the ends of the bar yields a transcendental equation involving: the resonant frequency, f; the Young's modulus parallel to the axis of the bar, E; the shear modulus, G, for the shear of one cross-section over another; and

quantities related to the dimensions of the bar. The transcendental equations for the various end conditions have been extensively studied from the point of view of predicting the resonant frequency if the dimensions and elastic moduli are known. For the present purpose, the problem is reversed: we wish to compute the value of one modulus from the measured resonant frequency and a known value of the other modulus. To make this computation economically for a large number of bars, a program was written for a digital computer.

The transcendental frequency equations for the various end conditions (free, supported, and clamped) have been derived by various authors; Huang[11] has derived the complete set*, and we shall start with his equation for the free-free bar. It is helpful to use a slightly more suggestive notation. Define dimensionless quantities

$$e = 4\pi^2 \rho f^2 L^2/E,$$

$$g = 4\pi^2 \rho f^2 L^2/kG,$$

and

$$a = A L^2/I,$$

where

ρ = density,

L = length of bar,

A = cross-sectional area,

I = moment of inertia of cross section about the principal axis perpendicular to the plane of vibration,

and k is a constant of order unity introduced by Timoshenko to take into account that the true distribution of shear stress over the cross section must be replaced by a single average value. For a specified bar in a particular mode of vibration, it is possible to find a value of k such that the solution of Timoshenko's equation is exact. The determination of the value of k to be used for a particular case is discussed in the next section. Note that e depends on E but not G and that g depends on G but not E. For round bars of diameter D,

$$a = 16 (L/D)^2;$$

* Since the derivations are rather long, it is, perhaps, worth recording that we have verified Haung's equations for the free-free and clamped-free bars.

and for a rectangular bar of cross-sectional dimension T in the direction parallel to the plane of vibration,

$$a = 12\,(L/T)^2.$$

For a bar with both ends free, the transcendental frequency equation is:

for $a > g$,

$$2\,(1-\cos\beta_1 \cosh\beta_2) + \frac{(e-g)^2 + 3\,ea-ga}{a\sqrt{e\,(a-g)}} \sin\beta_1 \sinh\beta_2 = 0$$

and, for $a < g$,

$$2\,(1-\cos\beta_1 \cos\beta_2) + \frac{(e-g)^2 + 3\,ea-ga}{a\sqrt{e\,(g-a)}} \sin\beta_1 \sin\beta_2 = 0,$$

where

$$\beta_1 = \left[\tfrac{1}{2}\,\left|\,\sqrt{(e-g)^2 + 4\,ea} + (e+g)\,\right|\right]^{1/2},$$

and

$$\beta_2 = \left[\tfrac{1}{2}\,\left|\,\sqrt{(e-g)^2 + 4\,ea} - (e+g)\,\right|\right]^{1/2}.$$

For specified values of f and G (or E), there are an infinite number of values of E (or G) which satisfy the transcendental equation, corresponding to the fact that the frequency might have been any member of the harmonic series. In order, so to say, to tell the computer how to find the correct root, it is necessary to have a detailed understanding of the nature of all the roots. It appears that the best way to consider the problem for the present purpose is to plot curves of ea versus g for a constant value of a, where the values of e, g, and a, corresponding to any point on a curve, satisfy Timoshenko's equation. For a given value of a (i.e., for a given bar), there are an infinite number of curves corresponding to the infinite number of harmonic vibrations of the bar. Figure 6 shows the first four solutions of Timoshenko's equation for values of a of 100, 1000, and infinity.

By using the definitions of e, g, and a, one can write the identity $ea = (ea/g)g$ in the form

$$ea = (kG\,AL^2/EI)\,g;$$

or, in terms of the quantities plotted in Figure 6,

$$\frac{ea}{10000} = \left(\frac{kG\;a}{100\,E}\right)\frac{g}{100}.$$

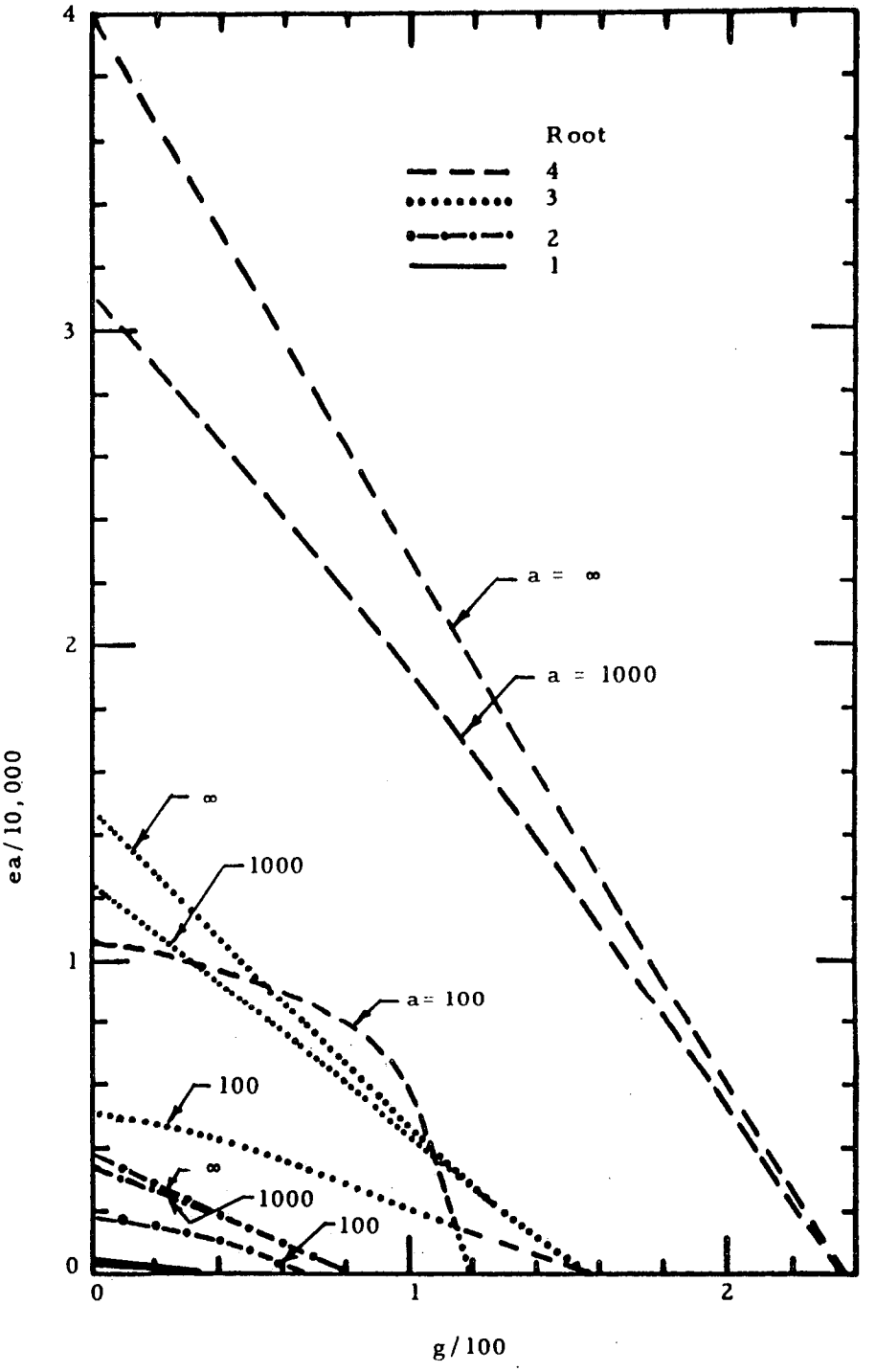

FIGURE 6. First Four Solutions of Timoshenko's Equation.

N-7165

The quantity in parentheses is independent of frequency; consequently, the values of ea and g for all the harmonic frequencies of a bar lie on a straight line through the origin with a slope which varies directly with kGa and inversely with E. The solutions of Timoshenko's equation are the intersections of this line with the curves of constant a of the type shown in Figure 6.

For the present problem, the value of the slope kGa/100E is not known initially. The computer program for the calculation of, say, E begins with the calculation of g and a. Then, the value of a function f (e, a, g), which is the left-hand side of the transcendental frequency equation, is computed for these values of g and a and at increasing multiples of a small increment Δea. Whenever a root has been passed, the value of the function f changes sign. After the proper number of sign changes to reach the root being sought, the precise value of e (and, hence, E) is calculated by a simple bracketing procedure. Figuratively, the computer process involves starting at the origin of Figure 6 and incrementing along the g axis by Δg, counting sign changes of f, to the required value of g. The next step is to increment parallel to the ea axis by Δea, counting sign changes, until the total number of sign changes equals the harmonic number of the resonant frequency. Then, the last root passed is determined with a prescribed precision. The program to calculate G is similar, but the iteration first goes up the ea axis to the known value of ea and then over to the right by increments on g.

Whether E or G can be determined accurately from a flexural vibration depends on the magnitude of the slope kGa/100E. Consider a rectangular bar with L/T = 10, for which a = 1200. For ordinary metals and polycrystalline graphite, kGa/100E is approximately 3 to 6. On drawing a line of this slope on Figure 6, one sees that a slight uncertainty in the slope* would cause only a small percentage error in the calculated value of E but a large percentage error in the value of kG. Therefore, in accordance with common practice, only Young's modulus E can be determined accurately from flexural vibrations of bars of most materials.

---

* In the computer program, the uncertainty, due to experimental error, is in the initial values of a and g (or ea); the effect of this uncertainty is the same as described in the text.

If the same size bar is made from compression-annealed pyrolytic graphite, kGa/100E is about 0.002 to 0.004 (in this case, G = c_{44}). A line of this slope on Figure 6 scarcely differs from the g/100 axis. A slight uncertainty in the slope would cause only a small percentage error in the calculated value of kG but a large percentage error in the value of E.

After neutron irradiation, it is expected that E will decrease slightly and G increase by a factor of about 10, yielding a value of kGa/100E of about 0.05. This value is still sufficiently small for a reasonably accurate value of kG to be determined from flexural vibrations. Thus, with the computer solution of Timoshenko's equation, it should be possible to follow the change in c_{44} with increasing neutron irradiation.

Determination of the Constant k

For ordinary materials, the shear contribution to the flexural motion is small, and it is not necessary to have a very precise value of k in order to calculate an accurate value of E from a resonant frequency. On the other hand, in determining the shear modulus, only the product kG can be determined; thus, the relative error in G will be as large as the relative error in k.

Pickett[12] has indicated that, for the fundamental flexural vibration of cylinders of ordinary materials, the best values of k are 0.833, 0.888, and 0.85 for Poisson's ratios, μ, of 0, $^1/_6$, and $^1/_3$; but there does not appear to be any information in the literature concerning the dependence of k on harmonic number or cross-sectional shape. These questions have been investigated both theoretically and experimentally.

The correct values of k for the first three harmonics (first harmonic = fundamental) and for several values of Poisson's ratio from 0.0 to 0.5 have been calculated for the flexural vibrations of isotropic round bars of various length to diameter ratios. The method of calculation was to use Tefft's[13] exact numerical solutions of the three-dimensional equations of elasticity together with our computer program to find the value of k for which Timoshenko's equation gives the exact solution. The results are given in Table 5, in which the values of G/E were computed from $G/E = 1/2(1+\mu)$. The trend of the first differences of the values of k throughout the table is occasionally erratic, suggesting that there may be a computational error of a few units in the fourth place.

TABLE 5

TIMOSHENKO'S CONSTANT k FOR FLEXURAL VIBRATIONS OF AN ISOTROPIC ROUND BAR

L/D	a	n*	μ = .5 G/E = .3333	.4 .3571	.3 .3846	.2 .4167	.1 .4545	.0 .5
50	40000	1	.9629	.9443	.9243	.9020	.8796	.8554
50	40000	2	.9642	.9451	.9249	.9036	.8808	.8568
50	40000	3	.9643	.9453	.9251	.9036	.8809	.8567
25	10000	1	.9642	.9451	.9254	.9040	.8814	.8575
25	10000	2	.9644	.9455	.9253	.9041	.8813	.8571
25	10000	3	.9644	.9455	.9254	.9038	.8810	.8568
10	1600	1	.9644	.9456	.9256	.9039	.8812	.8568
10	1600	2	.9647	.9461	.9260	.9044	.8811	.8562
10	1600	3	.9645	.9463	.9264	.9046	.8809	.8554
5	400	1	.9645	.9465	.9267	.9049	.8811	.8553
5	400	2	.9629	.9459	.9266	.9048	.8805	.8536
5	400	3	.9596	.9441	.9256	.9040	.8790	.8506

* n = harmonic number, n = 1 for fundamental

Two important conclusions can be drawn from the results given in Table 5. First, to within one per cent variation, the value of k is independent of harmonic number (at least up to n = 3) and of the length to diameter ratio. Second, as G/E increases from $^1/_3$ to $^1/_2$, the value of k decreases monotonically and does not, as Pickett suggests, pass through a maximum.

The effect of cross-sectional shape on the value of k has been investigated experimentally. The procedure was to measure several harmonics of the longitudinal, torsional, and two series of flexural vibrations (denoted by "D" and "T"), the planes of vibration of which were at right angles. The cross-sectional shapes were circular, square, and slightly rectangular. Aluminum, steel, fused silica, and as-deposited pyrolytic graphite were studied in order to have a range of G/E values.

The flexural vibrations were analyzed, using an iterative method of calculation: initially, a guess was made for the input values of the moduli and k for the computer program; then, moduli were calculated from the resonant frequencies and the input data. On the basis of this calculation, the input values of the moduli and k were adjusted; and the process was repeated until the moduli calculated from the different harmonics agreed, on the average, with the input values. It was found that a small error in the input value of E (or G) would cause a large error in the computed values of G for the first few harmonics (or of E for the higher harmonics). For isotropic materials,

this process determines unique values of E, G, and k. For materials of hexagonal symmetry and bars cut parallel to the basal plane, this process must be supplemented by an independent measurement of one of the four quantities c_{44}, c_{66}, and the two k values associated with these moduli. The ultrasonic value of c_{44} is a logical choice for this independent measurement.

For this initial work, the expense of high precision measurements was not justified. Consequently, the bars were prepared from standard stock by routine machining methods, and the measurements were made at room temperature. Slight anisotropy and nonhomogeneity were noted in the aluminum, steel, and quartz; since these effects are not of interest, the results were averaged in the following way. It was arbitrarily assumed the μ, G/E, and k were the same for both planes of flexural vibration; that is,

$$k = k_D = k_T$$

and

$$G_D/E_D = G_T/E_T.$$

To make the problem determinant, the average shear modulus, G, defined by

$$G = (G_D + G_T)/2,$$

was made equal to the value determined by the torsional vibrations. If an average Young's modulus, E, is defined by

$$E = (E_D + E_T)/2,$$

it follows that

$$G/E = G_D/E_D = G_T/E_T;$$

and the flexural vibrations determine a unique relation between k and G/E.

The tool steel square bar was the most homogeneous and isotropic; the complete results for this bar are given in Table 6 to illustrate the capability of the entire resonant bar system. It appears that the frequencies of the first and fourth torsional vibrations, the second flexural D vibration, and the first flexural T vibration are in error by about one part in five

thousand; but the rest of the data appears reliable. The value 0.873 ± .002 for k for a square bar is significantly less than the theoretical value of 0.923 for a round bar with the same value of G/E.

TABLE 6

RESULTS FOR TOOL STEEL FROM RESONANT BAR TESTS

Input Data

W = 503.94	gm	L/D = 16.049		G_D = 8.2970 x 10^{11} d/cm^2	
L = 25.473	cm	L/T = 16.023		G_T = 8.2870	
D = 1.5872	cm	G = 8.2920 x 10^{11} d/cm^2		E_D = 21.357	
T = 1.5892	cm	E = 21.344		E_T = 21.330	
		G/E = .38849		k = 0.873	

Output from Resonant Frequencies

Mode of Vibration	Harmonic	Modulus 10^{11} d/cm^2	Mode of Vibration	Harmonic	Modulus 10^{11} d/cm^2
Longitudinal	1	E 21.323	Torsional	1	G 8.2907
	2	E 21.300		2	G 8.2932
	3	E 21.245		3	G 8.2932
				4	G 8.2961
				5	G 8.2944
				6	G 8.2928
Flexural D Vibrations	1	E_D 21.357	Flexural T Vibrations	1	E_T 21.306*
	2	E_D 21.345*		2	E_T 21.330
	3	E_D 21.362		3	E_T 21.333
	4	E_D 21.357		4	E_T 21.329
	5	E_D 21.354		5	E_T 21.328
	6	E_D 21.350		6	E_T 21.335
	7	E_D 21.347		7	E_T 21.338
	Average	E_D 21.355		Average	E_T 21.332
	1	G_D 8.3125		1	G_T 7.5333*
	2	G_D 8.1867*		2	G_T 8.2835
	3	G_D 8.3186		3	G_T 8.3000
	4	G_D 8.2977		4	G_T 8.2840
	5	G_D 8.2918		5	G_T 8.2827
	6	G_D 8.2879		6	G_T 8.2935
	7	G_D 8.2866		7	G_T 8.2958
	Average	G_D 8.2992		Average	G_T 8.2899

* Value Omitted from Average.

Table 7 gives all of the experimentally determined values of k; and the data of Tables 5 and 7 are shown in Figure 7. The error assigned to k is only a rough estimate of the amount that k could be changed without making the flexural data for the bar strongly internally inconsistent. An important source of error which has not been estimated is nonhomogeneity within the bars. For the as-deposited pyrolytic graphite bars, the T plane of vibration is the basal plane [$G/E = c_{66}/(1/s_{11})$], and the D plane of vibration contains the c-axis [$G/E = c_{44}/(1/s_{11})$]. The values of k for the two round aluminum bars agree, within experimental error, with the theoretical values given in Table 5. The values for the isotropic square bars are all approximately 6 per cent less than the theoretical values for round bars.

Comparison of the isotropic square bars with the anisotropic rectangular pyrolytic bars raises two questions: how does k depend on the ratio of cross-sectional dimensions, D/T, of a rectangle and how does k depend on the degree of anisotropy? To investigate the first question, the values of k for rectangular and circular steel bars were calculated from the data of Spinner et al.[14,15] There is considerable scatter in the k values mainly because the values can be derived only from the fundamental resonance instead of from many harmonics. No dependence of k on the D/T ratio could be discerned; but, on the average, the value of k for rectangular bars was lower than that for circular bars. Essentially nothing is known about the effect of anisotropy on the value of k. However, for a rectangular bar of transversely isotropic material with one side parallel to the basal plane, there does not seem to be any reason why flexural vibrations in the D (or T) plane should depend, except in high-order corrections, on any of the elastic constants other than $1/s_{11}$ and c_{44} (or c_{66}). Therefore, for the present applications, it will be assumed that k depends on the appropriate G/E ratio but is otherwise independent of anisotropy.

The value of G/E for the D plane vibrations of compression-annealed pyrolytic graphite is approximately 0.0002. The data of Figure 7 for rectangular bars cannot be accurately extrapolated to this value of G/E, but a value of $k = 0.85 \pm .05$ seems indicated. From the results of this study, it follows that this value should apply to all harmonics, to all reasonable values of the D/T and D/L ratios, and to varying amounts of anisotropy.

TABLE 7

EXPERIMENTAL VALUES OF TIMOSHENKO'S CONSTANT k

Material	Sample Number	Shape	$\frac{L}{D}$	$\frac{L}{T}$	$\frac{G}{E}$	k
Aluminum	AL9-25	Round	36.17	——	0.3759	0.936 ± .005
	AL9-50	Round	18.02	——	.3718	.935 ± .005
	ALB200	Square	9.919	9.919	.3659	.874 ± .005
Tool Steel	TSB	Square	16.05	16.02	.3885	.873 ± .002
Fused Silica	FSB	Square	45.55	42.06	.4388	.832 ± .01
As-deposited Pyrolytic Graphite	M108-11	Rect.	9.136	6.441		
			D Plane of Vibration		.079	.88 ± .04
			T Plane of Vibration		.61	.70 ± .08
	P208-111	Rect.	20.41	15.72		
			D Plane of Vibration		.044	.86 ± .03
			T Plane of Vibration		.61	.73 ± .06

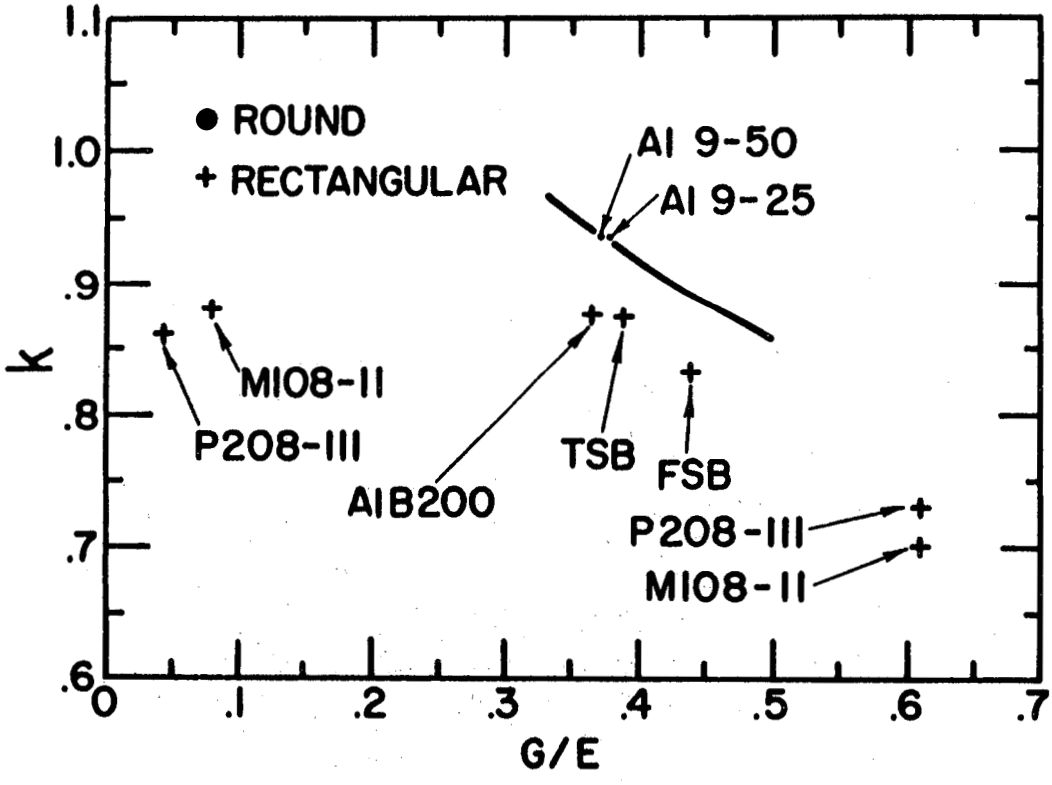

FIGURE 7. Timoshenko's Constant k Versus the Ratio of Shear to Young's Modulus. Solid Curve Gives Theoretical Values for an Isotropic Round Bar. N-7306

One experimental precaution is worth noting. For bars of weight less than approximately 5 grams and/or for frequencies less than approximately 5000 cps, it is essential that the bars be supported exactly at the displacement nodes and that the driver and receiver pickups be placed close to the nodes. Even with this precaution, the first few values obtained for harmonics of the flexural vibrations of long light bars were less accurate than those values for harmonics around the fifth. It is felt that the use of several harmonics is a valuable method of guarding against unexpected experimental errors in precision resonant bar work.

7.3. Results of Ultrasonic Tests

The accuracy of the ultrasonic measurement of c_{44} has been investigated by a transit time test. First, the transit time was measured on a sample, designated A, of compression-annealed pyrolytic graphite. Then, piece A was cleaved into three pieces, designated B, C, and D, and the transit time measured for each piece. Let t_j denote the transit time for piece j and Δt_{ij} denote the estimated transit time for the material lost in cleaning up the cleavage surfaces between pieces i and j. Then, the following relation should hold:

$$t_a = \Sigma t,$$

where

$$\Sigma t = t_b + t_c + t_d + \Delta t_{bc} + \Delta t_{cd}.$$

The experimental results are given in Table 8 for two samples of compression-annealed pyrolytic graphite. The measurements were made at one megacycle, for which the period is one microsecond. Since the difference between t_a and Σt is only about 0.1 microsecond, no error has been made due to the loss of the first cycle of the pulse or to an unknown phase reversal of the pulse. In thick (5 mm) samples, the error in c_{44} should be less than one per cent. In thin (0.5 mm) samples, for which there might be an additional 0.5 per cent error in measuring the thickness, the error in c_{44} should be less than two per cent. It is felt that similar estimates of error apply to the other elastic constants measured by ultrasonics.

The values of c_{44} for the various pieces are also given in Table 8. There is an appreciable variation through the original piece. This variation is rather surprising, especially in the propane material for which optical inspection of both the as-deposited and compression-annealed material had indicated a fairly uniform structure throughout the plate.

TABLE 8

ULTRASONIC RESULTS ON COMPRESSION-ANNEALED PYROLYTIC GRAPHITE

Piece	Measurement	Sample M110-3		Sample P210-3	
A	t_a	23.82	μs	18.68	μs
A+B+C	Σt	23.95		18.76	
A	c_{44}	0.0236 x 10^{11} d/cm^2		0.0297 x 10^{11} d/cm^2	
B	c_{44}	.0226		.0268	
C	c_{44}	.0231		.0297	
D	c_{44}	.0254		.0337	

7.4. Results of Resonant Bar Tests

The computer program has been used to analyze the resonant frequencies of several samples of compression-annealed pyrolytic graphite. As anticipated, the extreme anisotropy of this material imposes a restriction on the use of the flexural mode of vibration: it is unlikely that sufficiently accurate data will ever be available for $1/s_{66}$ to be determined from flexural T vibrations or for $1/s_{11}$ to be determined from flexural D vibrations. On the other hand, it has been found that inaccuracies in the input data cause variations in the $1/s_{11}$ determined from flexural T vibrations and in the k/s_{44} determined from flexural D vibrations both of which are small compared with the variability of these quantities from sample to sample. Consequently, the largest uncertainty in the analysis of the flexural vibrations is in the value of k to be used in calculating $1/s_{44}$.

One set of samples analyzed by the computer program is the four bars M103-11A, B, C, and D, for which some data has already been given in Table 5 of the Second Quarterly Report.[16] The new results for M103-11A and D (M103-11D is the designation given M103-11A after cutting a short length from each end) are given in Table 9; the results for the other two samples are similar. It will be noted that the value of $1/s_{44}$ given by the first flexural D vibration is about 5 per cent less than the values given by the higher harmonics. This situation has been noted on every bar that has been analyzed, the percentage difference usually being from 5 to 10. The low value given by the fundamental cannot be corrected by reducing the input value of $1/s_{11}$ by any reasonable amount. The cause of the variation is not known; possibly either there is a systematic experimental error or a different value of k should be used for the fundamental in this extreme limit of anisotropy.

TABLE 9

ELASTIC CONSTANTS OF COMPRESSION-ANNEALED PYROLYTIC GRAPHITE FROM RESONANT BAR TESTS

Sample	Mode of Vibration	Harmonic	Modulus 10^{11} d/cm^2	k
M103-11A	Flexural T	1	$1/s_{11}$ 66.5	
	D	1	$1/s_{44}$ .0178	0.89
	D	2	$1/s_{44}$ .0187	.89
	D	3	$1/s_{44}$ .0186	.89
	D	4	$1/s_{44}$ .0187	.89
	D	5	$1/s_{44}$ .0187	.89
	D	6	$1/s_{44}$ .0190	.89
	Torsional	1	$1/s_{44}$ .0209	
		2	$1/s_{44}$ .0773	
M103-11D	Flexural T	1	$1/s_{11}$ 69.9	
	D	1	$1/s_{44}$ .0176	0.90
	D	2	$1/s_{44}$ .0185	.90
	D	3	$1/s_{44}$ .0185	.90
	D	4	$1/s_{44}$ .0187	.90
	D	5	$1/s_{44}$ .0187	.90
	Torsional	1	$1/s_{44}$ .0201	
		2	$1/s_{44}$ .0880	

In this initial work, the value of k was chosen so that, on the average, the value of $1/s_{44}$ for the second and higher harmonics of the flexural D vibrations would be 0.0186×10^{11} d/cm^2. This value is in the middle of the range 0.0184 to 0.0189 given by ultrasonic and compound torsion oscillator tests on adjacent samples from the same plate.[17] The values of k necessary to give the "correct" value of $1/s_{44}$ for the four bars ranged from 0.88 to 0.90. These values of k are within the range predicted for this material in Section 7.2B. Further testing must be done to determine whether or not a value of k of 0.89 is applicable to other samples of compression-annealed pyrolytic graphite. However, it does appear certain that $1/s_{44}$ can be determined from flexural D vibrations with sufficient accuracy for the needs of the neutron irradiation program.

As indicated in Table 9, the value of $1/s_{44}$ given by the second torsional vibration is high by a factor of 3 or 4. This unexpected but complete failure of the torsional harmonic series ($n > 2$) of compression-annealed pyrolytic graphite has been found for every bar. The torsional vibrations are supposed to be described by a one-dimensional wave equation with an effective torsional modulus which depends on the bar dimensions and the elastic constants. However, the resonant frequencies are determined by the simple condition that the length of the bar be an integral number of half wave lengths; this condition leads to a series of harmonic frequencies which are integral multiples of the fundamental; that is,

$$f_n/n = f_1,$$

where f_n is the frequency of the n th harmonic. In isotropic materials, this condition is very accurately satisfied (see, for example, the data of Table 6). Table 10 gives the values of f_n/n for three rectangular bars of compression-annealed pyrolytic graphite which were obtained by cleaving an almost square bar into three pieces. It appears that as n increases, f_n/n first increases and then decreases, ultimately to below the value of the fundamental. (Differences in the fundamentals are due both to changes in the ratio D/T and to material differences.) Although the maximum amount of increase of f_n/n becomes less as the bar becomes thinner, there is no case for which the torsional harmonic series ($n > 2$) can be used with existing theory. A possible reason for this failure is that the motion may be a combination of torsion and plate shear modes

for which the resonant frequencies would be related to the elastic constants by a much more complicated theory than that used here.

It remains to be seen whether or not the fundamental torsional frequency is correct. The data of Table 9 indicate that the first torsional value of $1/s_{44}$ is high by 10 per cent, but this discrepancy might be due to material nonhomogeneity. In this extreme limit of anisotropy, the calculated value of $1/s_{44}$ is essentially independent of the input value of $1/s_{66}$. Although the value of $1/s_{44}$ deduced from the first torsional vibration may be in error by, perhaps, 10 per cent, this quantity is useful because it provides a check on the flexural value and because it should become more accurate as the material is irradiated and the shear modulus increases.

TABLE 10

VALUES OF f_n/n FOR THE TORSIONAL HARMONIC SERIES OF COMPRESSION-ANNEALED PYROLYTIC GRAPHITE

Harmonic	M106-2A D/T = 0.449	M106-2B D/T = 0.223	M106-2C D/T = 0.102
1	3952	3976	3686
2	5180	4489	3789
3	5712	4735	3813
4	5356	4782	3971
5		4394	3786
6		3935	3544
7			3332
8			3109
9			2918
10			2807
11			2680

8. PROPOSED IRRADIATION PROGRAM

The research program as originally outlined contained two parts:

Part One: A study of the mechanical properties of single crystal graphite and/or highly ordered pyrolytic graphite in the unirradiated state.

Part Two: An irradiation of selected samples of single crystals and pyrolytic graphite and the post-irradiation examination of these samples.

Although Part One is still in progress, sufficient data are now available to permit the planning of an irradiation program for the successful completion of the program as a whole. In the outline presented below, flexibility in each of the several aspects of the program is implied; subsequent revisions will be made as dictated by either pre-irradiation measurements or by parameters associated with the irradiation apparatus and the test reactor.

8.1. Irradiation Considerations

In many previous test programs, available test space has often dictated the choice of size and number of samples to be irradiated. Recognizing the expense of an irradiation program, it is essential that the sample number-test volume ratio be kept at a maximum. To this end, an objective of the pre-irradiation test program has been to determine the smallest sample sizes and the minimum number of samples required for an adequate statistical analysis of the post-irradiation measurements.

Of the several parameters to be considered from a scientific point of view, irradiation temperature and total neutron dose are the most important. Other parameters are related to the time necessary for irradiations, available reactor, test space, economics, and irradiation test rigs.

The temperature dependence of the damage is sufficiently well described by work on polycrystalline graphite that irradiation temperatures may be selected. Three temperatures have been chosen:

40°C, which is sufficiently high that inadvertent post-irradiation annealing will not be a severe problem in the experimental program. It is

also a temperature for which a large volume of data on polycrystalline graphite exist and below which temperature few terrestrial reactors will be operated.

250°C, a temperature which is just above the large annealing peak (200°C) and at which point the volume changes are near zero.

650°C, a representative temperature for the operation of several reactors and, again, a temperature at which much experimental data are available from polycrystalline graphite work.

The dose range is considered from two aspects: (1) the time available within the contract period for sample irradiation and post-irradiation examination and (2) the minimum dose at each selected temperature at which samples will incur a measurable and significant damage and the dose level at which saturation effects are expected to occur in single crystals of graphite.

8.2. Irradiation Program

A preliminary irradiation program in terms of temperature, accumulated flux (time), and number of irradiations is given in Table 11. Each capsule represented by an "X" is a volume 2.25 inches outside diameter and 4 inches long which contains the 47 samples which are described in Table 12.

TABLE 11

PROPOSED IRRADIATION SCHEDULE

Temperature °C	Radiation Level (MWD/AT)*											
	0.5	1	2	4	5	10	20	50	100	200	500	1000
40	x	x	x			x		x		x	x	
250		x	x		x		x		x		x	
650		x			x	x		x		x		x

* (1 MWD/AT = 1.7×10^{17} nvt at E > 0.18 Mev)

TABLE 12

DESCRIPTION OF SAMPLES FOR EACH IRRADIATION CAPSULE

Type Test	No. of Samples	Maximum Sample Dimensions
Sonic Resonant Bar	2	$^1/_4$" x $^3/_8$" x 3"
Ultrasonic	2	$^1/_2$" x $^1/_2$" x 2"
Ultrasonic	2	$^1/_8$" x $^3/_4$" x $^3/_4$"
Torsion CTO* (Sonic)	5	$^1/_2$" diameter x $^1/_4$" thick
Torsion (Static)	10	$^1/_2$" diameter x $^1/_4$" thick
Tensile	5	$^5/_8$" x $^3/_{16}$" x 3"
Compression (Static)	8	$^1/_2$" x $^1/_2$" x $^3/_8$"
Shear** 60° (Static)	3	$^1/_4$" x $^1/_4$" x $1^1/_8$"
Shear 45° (Static)	3	$^1/_4$" x $^1/_4$" x $^7/_8$"
Shear 30° (Static)	3	$^1/_4$" x $^1/_4$" x $^3/_4$"
Shear 15° (Static)	3	$^1/_4$" x $^1/_4$" x $^5/_8$"
Single Crystals	1	$^3/_4$" x 1" capsule

* Compound Torsion Oscillator

** Angles are the pitch of the wedge-shaped shear fixtures.

For 10^{14} nv fast flux, one-half MWD/AT per hour is an approximate conversion factor. It is immediately apparent that several of the irradiations will be much less than a reactor cycle; hence, retrieval of the capsules during reactor operation will be necessary. As an alternative, these capsules could be located at lower flux positions.

For 40°C irradiations, gamma heating may be a problem and temperature control may require special cooling for these irradiations. Except for the highest exposures (500 and 1000 MWD/AT), it may be possible to use a single rig for the 250°C and 650°C irradiations.

The time allotted for the irradiations and post-irradiation evaluation is one year, beginning April 1, 1965. In order to fit the irradiation program into this period, capsules should be ready for irradiation by April 1, and measurements of the post-irradiation mechanical properties must be carried out concurrently with the longer irradiations.

9. Future Work

The primary objective next quarter will be the completion of the pre-irradiation measurements for the pyrolytic graphite and graphite crystals.

Because of the difficulties associated with the tensile measurements on both compression-annealed and single crystal graphite, greater emphasis will be placed upon the measurement of the shear strength, the shear modulus, and the stress-strain diagram for between-the-planes shear. It is anticipated that single crystal shear-strength measurements will be completed next quarter; it is also anticipated that the possibility of measuring the in-plane stress-strain diagram for crystals in shear will be explored.

It will also be an objective of the work to produce more highly oriented pyrolytic graphite for the experimental program.

Plans for irradiations of both single crystal and compression-annealed pyrolytic graphite will be updated as the pre-irradiation evaluation progresses.

REFERENCES

1. Quarterly Progress Report No. 1, The Effects of Neutron Damage on the Mechanical Properties of Pyrolytic and Single Crystal Graphite, April 1, 1964 to June 30, 1964. (USAEC Contract No. AT-(40-1)-3237).

2. Quarterly Progress Report No. 2, The Effects of Neutron Damage on the Mechanical Properties of Pyrolytic and Single Crystal Graphite, July 1, 1964 to September 30, 1964. (USAEC Contract No. AT-(40-1)-3237).

3. E. N. Cameron and P. L. Weis, Strategic Graphite A Survey, United States Geological Survey Bulletin 1082-E, U.S. Government Printing Office, Washington, 1960.

4. D. E. Soule, Phys. Rev. 112, 699 (1958).

5. Private Communication.

6. op. cit., Quarterly Progress Report No. 2, p. 22.

7. Ibid., p. 26.

8. Ibid., p. 24.

9. Ibid., p. 30.

10. S. P. Timoshenko, Phil. Mag. 41, 744 (1921).

11. T. C. Huang, J. Appl. Mech. 28, 579 (1961).

12. G. Pickett, Proc. Am. Soc. Testing Materials 45, 846 (1945).

13. W. E. Tefft, J. Research National Bureau Standards 64B, 237 (1960).

14. S. Spinner, R. C. Valore, Jr. J. Research National Bureau of Standards 60, 459 (1958).

15. S. Spinner, T. W. Reichard, and W. E. Tefft, 64A, 147 (1960).

16. op. cit., Quarterly Progress Report No. 2, p. 38.

17. Ibid., p. 35-36.

DISTRIBUTION LIST

Reactor Division (3)
Oak Ridge Operations Office
U. S. Atomic Energy Commission
Post Office Box E
Oak Ridge, Tennessee

Fuels & Materials Development Branch (3)
Division of Reactor Development
U. S. Atomic Energy Commission
Germantown, Maryland

High Temperature Reactors Branch
Division of Reactor Development
U. S. Atomic Energy Commission
Germantown, Maryland

Division of Technical Information Ext. (3)
U. S. Atomic Energy Commission
Post Office Box 62
Oak Ridge, Tennessee

Pennsylvania State University
Attn: P. L. Walker, Jr.
University Park, Pennsylvania

Oak Ridge National Laboratory
Attn: B. L. Greenstreet
Post Office Box Y
Oak Ridge, Tennessee 37831

Argonne National Laboratory
Attn: Library
9700 South Cass Avenue
Argonne, Illinois 60440

General Electric Company
Nuclear Propulsion Operation
Attn: H. Wagner
Post Office Box 15132
Cincinnati, Ohio 45215

Brookhaven National Laboratory
Attn: D. Gurinsky
Upton, New York 11973

General Electric
Hanford Atomic Products Operation
Attn: R. Nightingale
Post Office Box 100
Richland, Washington

General Atomics
Division of General Dynamics Corp.
Post Office Box 608
Attn: W. Goddell
San Diego, California 92112

Library (T. D. S.)
Jet Propulsion Laboratory
California Institute of Technology
4800 Oak Grove Drive
Attn: N. E. Devereux,
Library Supervisor
Pasadena, California 91103

Union Carbide Corporation